DOI:
10.1182/blood-2017-07-794784

Document Version
Peer reviewed version

Pml nuclear body disruption cooperates in APL pathogenesis, and impairs DNA damage repair pathways in mice

Edwige Voisset[1], Eva Moravcsik[1], Eva W. Stratford[2], Amie Jaye[1,3], Christopher J. Palgrave[4], Robert K. Hills[5], Paolo Salomoni[6,7], Scott C. Kogan[8], Ellen Solomon[1] and David Grimwade[1§]

[1]Department of Medical & Molecular Genetics, King's College London, Faculty of Life Sciences & Medicine, London, United Kingdom;
[2]Department of Tumor Biology, The Norwegian Radium Hospital, Oslo University Hospital, Oslo, Norway;
[3]Present address: Department of Life Sciences, Imperial College London, London, United Kingdom;
[4]School of Veterinary Medicine, University of Surrey, Guildford, United Kingdom;
[5]Centre for Trials Research, College of Biomedical & Life Sciences, Cardiff University, Cardiff, United Kingdom;
[6]UCL Cancer Institute, London, United Kingdom;
[7]Present address: German Center for Neurodegenerative Diseases (DZNE), Bonn, Germany;
[8]Helen Diller Family Comprehensive Cancer Center & Department of Laboratory Medicine, University of California, San Francisco, CA, USA.
§ Deceased.

To whom correspondence should be addressed:
Dr Edwige Voisset & Prof Ellen Solomon
Department of Medical and Molecular Genetics
King's College London, Guy's Hospital, Floor 8, Tower Wing
London SE1 9RT, UK
Phone: +44 (0) 207 848 8146
Fax: +44 (0) 207 188 2585
E-mail: edwige.voisset@kcl.ac.uk and ellen.solomon@kcl.ac.uk

Conflict of interest:
The authors declare no competing financial interests.

Running title: Role of Pml nuclear bodies in APL pathogenesis

Scientific Category: Myeloid Neoplasia

Character count:
Text word count: 3953;
Abstract word count: 197;
Number of figures: 6;
Number of references: 87.

KEY POINTS

- A novel mouse model elucidates the impact of Pml NB disruption on APL pathogenesis and response to targeted therapy.

- The mode of action of this disruption appears to be via the perturbation of the NHEJ and HR pathways.

ABSTRACT

A hallmark of acute promyelocytic leukemia (APL) is altered nuclear architecture, with disruption of PML nuclear bodies (NBs) mediated by the PML-RARα oncoprotein. To address whether this phenomenon plays a role in disease pathogenesis, we generated a knock-in mouse model with NB disruption mediated by two point mutations (C62A/C65A) in the Pml RING domain. While no leukemias developed in $Pml^{C62A/C65A}$ mice, these transgenic mice also expressing RARα linked to a dimerization domain (p50-RARα model) exhibited a doubling in the rate of leukemia, with a reduced latency period. Additionally, we found that response to targeted therapy with all-*trans* retinoic acid (ATRA) in vivo was dependent on NB integrity. PML-RARα is recognized to be insufficient for development of APL, requiring acquisition of cooperating mutations. We therefore investigated whether NB disruption might be mutagenic. Compared to wild-type cells, primary $Pml^{C62A/C65A}$ cells exhibited increased sister-chromatid exchange and chromosome abnormalities. Moreover, functional assays showed impaired homologous recombination (HR) and non-homologous end-joining (NHEJ) repair pathways, with defective localization of Brca1 and Rad51 to sites of DNA damage. These data directly demonstrate that Pml NBs are critical for DNA damage responses, and suggest that Pml NB disruption is a central contributor to APL pathogenesis.

INTRODUCTION

Acute promyelocytic leukemia (APL) is one of the commonest subtypes of acute myeloid leukemia (AML), with the vast majority of cases harboring the t(15;17) chromosomal translocation, involving the fusion of the genes encoding PML (promyelocytic leukemia) and the transcription factor RARα (retinoic acid receptor alpha)[1-3]. The outcome for APL patients has been transformed with the advent of molecularly-targeted therapies, i.e. arsenic trioxide (ATO) and all-*trans* retinoic acid (ATRA), which bind to the PML and RARα moieties of PML-RARα, respectively. These two drugs act in synergy to trigger PML–RARα degradation, by promoting apoptosis (ATO) and cellular differentiation (ATRA), inducing clinical remission[4-7].

PML is localized in PML nuclear bodies (NBs)[8-10], discrete subnuclear structures of which PML is a crucial component[11-13]. Indeed, PML not only promotes NB biogenesis and maintains its integrity[3,14,15], but is also involved in the recruitment and localization of approximately one hundred proteins into this complex (e.g. SUMO-1, CBP, DAXX, BLM)[16]. The post-translational modifications of PML, including its SUMOylation, are critical steps in the formation of mature PML NBs[3,17-19]. PML NBs are dynamic multiprotein complexes[16], involved in various major processes such as stem cell self-renewal, cell death, and transcription[20].

Cells utilize different DNA repair pathways depending on the type of damage, and the phase of the cell cycle in which the damage occurs. DNA double-strand breaks (DSBs) produced by ionizing radiation (IR), for example, can be repaired by two major mechanisms: the non-homologous end joining (NHEJ) and homologous recombination (HR) repair pathways. NHEJ, which is mostly active during the G1 phase of the cell cycle, mediates direct ligation of the broken DNA ends in an error

prone manner. HR is, by contrast, largely error free, and arises in the G2 phase using sister chromatids as templates for repair. Failure in DNA DSB repair may lead to genomic instability, and consequently cancer predisposition[21].

Numerous studies have highlighted the importance of the capacity of the PML-RARα fusion protein to oligomerize (conferred by the PML moiety) in APL pathogenesis , in contrast to wild-type RARα which lacks this property[22,23]. Moreover, it is also unambiguous that PML-RARα expression has a major impact on nuclear architecture leading to NB disruption into nuclear microspeckles, which is a diagnostic hallmark of APL[3]. This phenomenon has been proposed as a key step in leukemogenesis[24], but this has not been formally explored in vivo until now. Furthermore, NB disruption is reversed by ATO or ATRA treatment[25], suggesting that normalization of nuclear architecture may be important for response to targeted therapies. To address these issues, we have generated a novel knock-in mouse model, where targeted Pml NB disruption was achieved through mutation of two key zinc-binding cysteine residues (C62A/C65A) in the RING domain of Pml. Our mouse model highlights the essential cooperative role of the NB disruption induced by PML-RARα expression in APL development, and the importance of re-formation of NBs in generating an efficient response to differentiating drug (ATRA). Additionally, our data reveal that Pml NBs are determinants of the quality of DNA damage repair via both NHEJ and HR repair pathways.

MATERIALS AND METHODS

Animal experimental guidelines

All animal experimentations were performed in accordance with the terms of UK Home Office guidelines. The home office project license number under which these experiments were conducted is PPL 70/7720.

Transplantation experiments

All transplant recipient mice were 8-12 weeks old at the time of transplantation. Unfractionated BM cells ($0.5–1\times10^6$) were transplanted into sublethally irradiated mice (4.5 Gy) via tail vein injection. PML-RARα leukemic BM cells were transplanted into sub-lethally irradiated FVB/N Hsd mice. Moribund mice were humanely sacrificed, and leukemia was routinely confirmed by May-Grünwald Giemsa staining, peripheral blood analyses or independently confirmed by a veterinarian.

Leukemia samples used for transplantation experiments were as follows: #1707, #M1/28, and #1787 for Pml^{WT}+p50-RARα; #1403, #626, and #628 for $Pml^{C62A/C65A}$+p50-RARα; #1111/3, #935/5, and #1097/1 for PML-RARα.

For ATRA in vivo-experiments, placebo or ATRA 21-day release pellets (5 mg; Innovative Research of America) were subcutaneously implanted 7 days post-transplantation as per manufacturer's instructions.

Immunoprecipitation and immunoblot analysis

Cells were lysed on ice in RIPA buffer containing protease inhibitor cocktail (Roche) and 20 mM NEM (Sigma-Aldrich). Lysates were pre-cleared with Sepharose 4B

beads (GE Healthcare), and then immunoprecipitated with the relevant antibody or isotype control as previously described[26]. Immunoprecipitates and whole cell lysates were separated by SDS-PAGE and transferred to PVDF membranes (Millipore). Membranes were blocked in 5% BSA, and then incubated with primary antibodies overnight at 4ºC. Immunodetection was performed using ECL Western blotting substrate (ThermoFisher), or using infrared imaging (Odyssey LI-COR).

Flow cytometry assays

LSK population was defined as previously described[27]. Briefly, lineage-depleted (Dynabeads, ThermoFisher) BM cells were stained with fluorochrome-conjugated antibodies against Sca-1, and c-Kit (Biolegend), and the lineage cocktail (B220, CD3, CD4, CD8, Ter119, Mac-1, and Gr-1; Biolegend). CD11b/Gr-1 population analysis was performed as previously described[28]. Flow cytometry was performed on a BD LSRFortessa cell analyzer and data were analyzed with FlowJo software (Tree Star).

In vivo cell cycle analysis

Mice were injected with 50 mg/kg EdU (5-ethynyl-2'-deoxyuridine) 2 h before BM harvest[29]. Cells were processed using a Click-iT EdU Flow Cytometry Assay kit (ThermoFisher).

Nitro blue tetrazolium (NBT) reduction assay

0.1% of NBT (Sigma-Aldrich) was added to leukemic BM cells on poly-D-lysine coated coverslips, and incubated in a 5% CO_2 incubator at 37°C. Images were taken under Eclipse Ti-E Inverted Imaging System (Nikon), and auto-analyzed with the NIS software. At least 1100 cells were counted per sample.

NHEJ and HR activity assay

All cell types were nucleofected using Amaxa kit (Lonza) following the manufacturer's instructions. Briefly, cells were co-transfected with linearized NHEJ reporter plasmid or linearized HR reporter plasmid (kind gifts of Dr Vera Gorbunova; U. Rochester) and pDsRed-Express-N1 plasmid (Clontech; as transfection efficiency control) as previously described[30,31]. Lineage-depleted BM cells were isolated 12 h before nucleofection[32]. Flow cytometry was performed on a BD LSRFortessa cell analyzer and data were analyzed with FlowJo software (Tree Star).

RESULTS

Generation of a Pml$^{C62A/C65A}$ knock-in mouse model, and Pml$^{C62A/C65A}$+p50-RARα mice

To investigate the functional consequences of Pml NB disruption, we engineered a knock-in mouse model by substituting two zinc-binding cysteine residues for two alanine residues located in the RING domain at positions 62 and 65, via site-directed mutagenesis and subsequent homologous recombination in mouse ES cells (**supplemental Figure 1A-E**). For simplicity, homozygous mutant mice will be referred to as Pml$^{C62A/C65A}$. Pml$^{C62A/C65A}$ mice are developmentally normal, and do not die of spontaneous leukemias or tumors.

The importance of RARα dimerization in APL pathogenicity has been reported previously[33]. To explore whether RARα dimerization operates conjointly with NB disruption, Pml$^{C62A/C65A}$ mice were crossbred with p50-RARα transgenic mice[34], in order to generate Pml$^{C62A/C65A}$+p50-RARα mice; here, RARα dimerization is artificially forced by linking to the dimerization domain of the NF-κB p50 subunit[33,34]. All the mouse models used in this study have been color-coded, as summarized in **supplemental Figure 1F**.

Pml$^{C62A/C65A}$ expression causes dispersion of NB constituents, deficiency of Pml SUMOylation, and expansion of the LSK compartment

We next investigated whether endogenous Pml$^{C62A/C65A}$ expression induced Pml NB disruption, as previously described when overexpressed in human cell lines[15,35,36]. We performed immunofluorescence staining to analyze the localization of well-known NB constituents. Initially, Pml staining was used as a first-line control of Pml NB

disruption; this confirmed that $Pml^{C62A/C65A}$ was dispersed in primary mouse embryonic fibroblasts (MEFs) compared to wild-type Pml (Pml^{WT}). Additionally, while Daxx, Cbp and Sumo-1 formed clear and bright foci in Pml^{WT} MEFs, a diffuse nuclear pattern was observed in $Pml^{C62A/C65A}$ and $Pml^{-/-}$ cells[17,37] (**Figure 1A**). We confirmed that these differences did not result from variations in the level of protein expression (**Figure 1B**). The $Pml^{C62A/C65A}$ mutant replicated the NB disruption seen in primary human APL cells, with dispersion of PML and NB constituents (e.g. DAXX), and as shown in the PML-RARA-expressing NB4 human cell line. As expected, treatment of NB4 cells with ATRA led to re-localization of DAXX and PML into NBs[38] (**Figure 1C**).

The PML RING domain is essential for PML SUMOylation[14,15,37,39]. Immunoprecipitations of Sumo-1 or Sumo-2/3 revealed that endogenous Pml^{WT} was SUMOylated in MEFs at basal level, and hyper-SUMOylated following ATO treatment (**Figure 1D**). Moreover, post-ATO treatment, Pml^{WT} was found to be ubiquitinated. None of these smears of bands were detected in $Pml^{C62A/C65A}$ cells, or as expected in $Pml^{-/-}$ cells (negative control)[26] (**Figure 1D**). Collectively, we confirmed that the C62A/C65A mutation induces NB disruption in a fashion similar to that observed in the context of PML-RARα. These data also demonstrate that the integrity of the RING domain is required not only for PML SUMOylation, but also for the ATO induced-PML degradation pathway.

In vivo, $Pml^{C62A/C65A}$ mice did not exhibit alterations in peripheral blood count parameters. However, the number of $Lin^{-}Sca\text{-}1^{+}c\text{-}Kit^{+}$ (LSK) hematopoietic stem and progenitor cells was greatly increased, and this increase was even more significant than that seen in the absence of Pml (i.e. $Pml^{-/-}$ mice) (**Figure 1E**; **supplemental Figure 2**). Cell cycle analysis revealed that the higher number of LSK cells in

$Pml^{C62A/C65A}$ mice, and to a lesser extend in $Pml^{-/-}$ mice, was attributable, at least in part, to an acceleration of cell cycle progression (**Figure 1F-G**). Unlike LSK cells, Pml^{WT}, $Pml^{-/-}$ and $Pml^{C62A/C65A}$ primary MEFs did not present any variations in their cell cycle nor cell death profiles (**supplemental Figure 3**), thus making MEFs a more suitable model to analyze downstream cellular functions.

Pml NB disruption promotes APL pathogenesis

While no disease was detected over an 18-month observation period in Pml^{WT} (0/249) or $Pml^{C62A/C65A}$ (0/251) mice, both Pml^{WT}+p50-RARα (15/252) and $Pml^{C62A/C65A}$+p50-RARα (32/251) mice developed APL spontaneously (**Figure 2A-B**). These leukemias were characterized by hyperleukocytosis, anemia and thrombocytosis, and validated by post-mortem examination revealing, for example, pale bone marrow (BM) and splenomegaly (mean weight of healthy adult spleen, 25.75 mg; Pml^{WT}+p50-RARα leukemic spleen, 458 mg; $Pml^{C62A/C65A}$+p50-RARα leukemic spleen, 642 mg; PML-RARα leukemic spleen as control, 580 mg). The cumulative incidence of APL differed significantly between Pml^{WT}+p50-RARα and $Pml^{C62A/C65A}$+p50-RARα genotypes, with a frequency at 18 months of 6.8% and 13.8%, respectively, leading to a penetrance comparable to that observed in PML-RARα transgenic models[40-42] (**Figure 2A**). Moreover, the latency period before the onset of leukemia was significantly reduced in the context of NB disruption compared to Pml^{WT}+p50-RARα (to 213 days of age versus 310 days; $p<0.008$; **Figure 2A**). These results demonstrate cooperativity between NB disruption and RARα dimerization in the initiation of APL.

We then assessed APL-initiating activity by transplanting primary APL-derived cells into recipient mice. The vast majority of mice transplanted with leukemic

Pml^{WT}+p50-RARα (11/14) or Pml$^{C62A/C65A}$+p50-RARα (6/8) unsorted BM cells developed APL (**Figure 2C**). The latency period to disease was similar to that previously observed upon transplantation of PML-RARα leukemic blasts[40]. None of the mice which received a mock transplant (PBS) developed any disease. Secondary and tertiary transplants of unsorted BM cells retained the capacity to initiate APL for these three genotypes.

The similarities we observed between Pml$^{C62A/C65A}$+p50-RARα and PML-RARα mice thus strengthen evidence for the crucial contribution of Pml NB disruption to APL pathogenesis.

Pml NBs are involved in the response to ATRA treatment

Induction of myeloid differentiation is the hallmark of response to ATRA[43]. To analyze the effect of NB disruption on ATRA-induced differentiation, we firstly performed an in vitro NBT assay. When unsorted leukemic BM cells, isolated from recipients transplanted with PML-RARα or Pml^{WT}+p50-RARα cells, were incubated with ATRA, the percentage of differentiated cells was greatly enhanced compared to cells treated with the vehicle control (DMSO) (**Figure 3A**). Interestingly, Pml$^{C62A/C65A}$+p50-RARα cells treated with ATRA did not present a significant increase in the percentage of differentiated cells (**Figure 3A**). The absence of granulocytic differentiation following ATRA exposure in Pml$^{C62A/C65A}$+p50-RARα-derived APL cells was confirmed by analysis of CD11b and Gr1 expression (**Figure 3B**). In vivo, ATRA-treated mice post-transplantation also confirmed these results: survival was significantly improved only for PML-RARα and Pml^{WT}+p50-RARα transplanted mice, compared to placebo-treated mice (**Figure 3C**). These data reveal

the importance of Pml NB re-formation for an effective response to the differentiating drug.

Pml NBs are involved in the maintenance of genome integrity and essential for optimal DNA DSB repair via the NHEJ and HR pathways

The *PML-RARA* translocation is undoubtedly an initiating event in APL pathogenesis, but is not sufficient by itself for the full development of APL. Indeed, it is now well-established that APL is a multistep disease, requiring additional cooperating mutations, thus explaining the long latency period prior to leukemia onset[44-48]. To determine whether the three different genotypes generated APL with similar mutational spectra, we performed whole-exome sequencing on samples from Pml^{WT}+p50-RARα and $Pml^{C62A/C65A}$+p50-RARα spontaneous leukemias, and on PML-RARα transplant samples. Interestingly, some of the mutated genes were common to human APL (e.g. *Kras*, *Ptpn11* and *Usp9y*) or human AML (e.g. *Pten* and *Jak2*)[48-51], and some of the copy number variants were common to human APL/AML (e.g. *Kdm6a* and *Ezh2*) or human myelodysplastic syndromes (e.g. *Cul1*)[46,52,53] (**supplemental Figure 4 and supplemental Table 1**).

Then, we speculated that loss of NB integrity might affect DNA DSB repair pathways[13,54]. To investigate the efficiency of the NHEJ and HR pathways, we used a well-established system of reporter assays[30,31]. $Pml^{-/-}$ primary MEFs did not exhibit any defect in the NHEJ pathway when compared to Pml^{WT} cells (**Figure 4A and supplemental Figure 3A**). They did, however, present a significant reduction in the efficiency of the HR pathway, as previously reported[13]. Strikingly, both NHEJ (with Compatible and Incompatible DNA ends) and HR pathway activities were diminished in $Pml^{C62A/C65A}$ MEFs. Similar results for the NHEJ pathway have been obtained with

lineage-depleted BM cells isolated from the Pml$^{C62A/C65A}$ mouse model, compared to Pml^{WT} (**Figure 4B**). The forced dimerization of RARα also affected the efficiency of the NHEJ pathway to a level similar to that observed in Pml$^{C62A/C65A}$ cells (**Figure 4B**). Moreover, an additive effect was observed in Pml$^{C62A/C65A}$+p50-RARα cells compared to Pml^{WT}+p50-RARα cells (**Figure 4B**). Importantly, similar results were obtained with an inducible PML-RAR⍁-expressing cell line (**Figure 4C**), thus reinforcing the resemblance observed between Pml$^{C62A/C65A}$– and PML-RARα–induced NB disruption.

To determine whether these defects in DNA DSB repair pathways were due to a reduced kinetics of repair and/or reduced quality of repair, we analyzed MEF metaphase spreads. First, these revealed a significantly greater number of chromosome aberrations in Pml$^{C62A/C65A}$ cells in response to ionizing radiation (IR), compared to Pml^{WT} and Pml$^{-/-}$ cells (**Figure 4D**). Second, a significantly higher number of spontaneous sister chromatid exchange (SCEs) was also found in Pml$^{C62A/C65A}$ cells, compared to WT cells (**Figure 4E**). Additionally, the rate of SCE formation in Pml$^{C62A/C65A}$ cells was similar to that observed in Pml$^{-/-}$ cells.

Altogether, these data indicate that NB dispersion gives rise to a higher level of recombination activity in primary cells, and further suggests that mice lacking Pml NBs may have an unstable genome.

Investigation of the defective NHEJ pathway in Pml$^{C62A/C65A}$ cells uncovers 53BP1 and Brca1 alteration

We tracked the time-course of γH2AX foci formation and disappearance, a well-established indicator of DNA DSBs, in MEFs and in lineage-depleted BM cells, pre- and post-IR exposure (**supplemental Figure 5 and 6A-B**). An obvious induction of

γH2AX foci was observable 1 h post-IR, compared to untreated cells. The kinetics of repair were identical for all genotypes studied (**supplemental Figure 6A-B**). This result was confirmed by Western blot analyses, since equivalent levels of γH2AX, between genotypes, were observed at each time point (**supplemental Figure 6C**).

Examining the NHEJ pathway-specific factors, we found that the number of 53BP1 foci was altered in $Pml^{C62A/C65A}$ MEFs, with no variation in protein expression (**Figure 5A, supplemental Figure 6C and 7**). Indeed, $Pml^{C62A/C65A}$ MEFs presented significantly more 53BP1 foci in the context of spontaneous DNA lesions, when compared to Pml^{WT} and $Pml^{-/-}$ cells. 53BP1 was found to co-localize normally with γH2AX, as shown in **Figure 5B**. 53BP1 and Brca1 are central in the regulation of the balance between NHEJ and HR pathways[55]. Interestingly, following IR exposure, 53BP1 and Brca1 foci co-localized at a higher level in $Pml^{C62A/C65A}$ MEFs (mean: 43.81%) compared to Pml^{WT} and $Pml^{-/-}$ cells (mean: 25.27% and 25.82% respectively; **Figure 5C-D**). These data revealed that Pml NB integrity is required for correct functional crosstalk between DNA repair proteins involved in the switch between NHEJ and HR pathways. Consequently, the erroneous localization of Brca1 in $Pml^{C62A/C65A}$ cells may also be part of the disturbance observed in the HR pathway.

Investigation of the defective HR pathway reveals the importance of Pml NB integrity for the correct localization of Rad51 at DSBs

We then analyzed two main factors of the HR pathway: Blm and Rad51. Unfortunately, none of the commercial antibodies tested against Blm produced positive signals in immunofluorescence assays. As a surrogate, we therefore overexpressed GFP-Blm in primary MEFs (**Figure 6A**). In order to determine whether overexpressed Blm accumulates in a fashion similar to the endogenous

protein, co-staining with Pml was performed in wild-type cells. As expected, Blm and Pml co-localized[56] (**Figure 6B**). In a similar manner to 53BP1, the number of foci for Blm and Rad51 differed at basal level, reflecting a disturbance in the HR pathway in $Pml^{C62A/C65A}$ and $Pml^{-/-}$ MEFs, compared to Pml^{WT} cells (**Figure 6C-D**, **supplemental Figure 8 and 9**). When protein localization was analyzed, no mislocalizations were observed for Blm foci. Regarding Rad51, confocal analyses revealed strikingly that Rad51 minimally co-localized with γH2AX in $Pml^{C62A/C65A}$ and $Pml^{-/-}$ cells, compared to Pml^{WT} MEFs (**Figure 6E**). These observations were validated by co-immunoprecipitation experiments. Notably, while the same amount of Rad51 was immunoprecipitated, the amount of γH2AX pulled down was lower in $Pml^{C62A/C65A}$ and $Pml^{-/-}$ compared to Pml^{WT} lysates (**Figure 6F**).

Collectively, our data provide further evidence that Pml NBs are essential for effective DNA repair response, and that their disruption is in part responsible for the deficiency observed in the context of PML-RARα expression.

DISCUSSION

APL development is invariably associated with translocations of the *RARA* gene, and numerous studies have been carried out to determine how the resulting fusions contribute to the pathogenesis of this disease. These include studies of the importance of the fusion partners, but these have been directed more towards their oligomerization potential. As a result, the role played by Pml NB disruption in APL pathogenesis had not been studied in a comprehensive way. Nevertheless, two particular studies have provided preliminary evidence for the importance of Pml NB disruption in leukemogenesis. Using truncated versions of the PML-RARα fusion protein, they hypothesized that the PML moiety was required not solely for the dimerization of RARα, and that the observed Pml NB disruption might play an active role in APL pathogenesis[57,58]. Here, we used a novel knock-in mouse model, in which Pml NBs are disrupted in a similar fashion to that observed in the context of PML-RARα expression, in order to dissect their impact.

Using this model, we showed definitive evidence for the involvement of Pml NB disruption in APL initiation, in synergy with the forced dimerization of RARα. We also showed that an effective response to ATRA treatment requires Pml NB integrity. These data validate the proposed hypothesis that NBs contain essential factors for nuclear hormone receptor signal transduction[11,59,60], and demonstrate that the wild-type Pml allele plays an important role in tumor regression following ATRA treatment for PML-RARα APL[61]. These points are of importance since ATRA and its derivatives are under investigation not only for the treatment of other AML subtypes[62,63], but also for other malignancies[64-68]. Furthermore, Pml$^{C62A/C65A}$+p50-

RARα mouse model recapitulates substantially APL pathogenesis as observed in PML-RARα APL mouse models.

Previous studies have investigated the connection between Pml NBs and DNA damage repair. However, owing to the models used, PML-RARα[54,69] or $Pml^{-/-}$ cells[13,70], it was impossible to establish a direct link between the two. On the one hand, the consequences of disruption could not be disassociated from those due to alterations in the RARα signaling; on the other hand, the absence of *Pml* expression is not necessarily equivalent to Pml mislocalization and Pml NB disruption, as it has been exemplified in this study. Indeed, we report here that both NHEJ and HR repair pathways are drastically altered by the loss of Pml NB integrity, while only the HR pathway was impaired in $Pml^{-/-}$ cells. Repair through NHEJ was considerably more altered in $Pml^{C62A/C65A}$+p50-RARα cells than in $Pml^{C62A/C65A}$ or Pml^{WT}+p50-RARα cells, revealing that Pml NB disruption and the forced dimerization of RARα had a cooperative effect on DNA damage responses. Surprisingly, no alterations in the kinetics of repair following IR exposure were noticeable, since clearance of γH2AX foci was similar in all genotypes analyzed. Based on these results, it was possible to refute the hypothesis that the higher number of γH2AX foci observed in PML-RARα cells[71] is exclusively due to Pml NB dispersion[69,70]. Also, PML-RARα is able to initiate leukemia, but additional events are needed to lead to complete leukemic transformation as observed in various transgenic mouse models[40-42]. It is thus plausible that the acquisition of cooperating mutations[46,72] is facilitated by the loss of Pml NB integrity. This hypothesis is further strengthened by published reports, which have established that the majority of de novo mutations are random events in AML/APL[48-50].

The NHEJ and HR pathways involve a large number of different factors, including 53BP1 for the NHEJ pathway, and Brca1, Blm and Rad51 for the HR pathway[21]. Here, we found an excess of 53BP1, Blm and Rad51 foci in Pml$^{C62A/C65A}$ cells compared to Pml^{WT} cells. Interestingly, in recent years, SUMO and ubiquitin signals have been characterized as essential components in DNA damage responses[55,73], and indeed, deficient SUMOylation of Blm and/or Rpa has been shown to impair Rad51 localization[74-76]. Our results, therefore, suggest a scenario in which the putative incorrect SUMOylation of Blm and/or Rpa (due to SUMOs being inadequately localized in Pml$^{C62A/C65A}$ cells) might partially explain our observation of Rad51 mislocalization. 53BP1 foci, which were found in excess only in the context of Pml$^{C62A/C65A}$ expression, were still located at sites of damage, suggesting that the DNA DSB-specific histone signature, including ubiquitination, is not affected by Pml NB disruption[77]. It would be of interest, therefore, to carry out further analyses of 53BP1 phosphorylation, the localization of its partners (e.g. Rif1), and indubitably the SUMOylation of 53BP1 itself[78,79], in order to establish the causes and consequences of this excess of 53BP1 foci. Moreover, 53BP1 dysregulation might also have repercussions in the HR pathway, since 53BP1 and Brca1 are key regulators of the balance between NHEJ and HR repair pathways during the S-G2 phases of the cell cycle[80-84]. Also, the SUMO pathway is an important regulator of Brca1 functions[85-87]. Finally, the discrepancies observed between the absence of Pml NBs and their disruption (i.e. Pml$^{-/-}$ versus Pml$^{C62A/C65A}$ mutants) could also be linked to their distinct impact on Sumo-2/3: while Sumo-2/3 formed abnormally large foci in Pml$^{-/-}$ cells, a diffuse pattern was observed in Pml$^{C62A/C65A}$ cells (**supplemental Figure 10A**). These data are consistent with the role of Pml as a dynamic anchor regulated by SUMOylation[3,16]. Indeed, since Pml is expressed in Pml$^{C62A/C65A}$ cells, and because

the SUMOylome is severely reduced but still extant (**supplemental Figure 10B-E**), some proteins could still be recruited by Pml through its SUMO-interaction motif (SIM), for example, and might subsequently become sequestrated and/or mislocalized. In accordance with this hypothesis, our finding that 53BP1 SUMOylation was not affected in the same way in $Pml^{-/-}$ and $Pml^{C62A/C65A}$ cells could explain, at least partially, the disparity observed in the NHEJ pathway (**supplemental Figure 10F-G**). Thus, further study is needed to establish whether Pml NB disruption significantly affects the SUMOylome, and its potential downstream impacts on DNA damage responses (**supplemental Figure 10 and 11**).

Overall, we found strong evidence for the essential pathogenic role of PML-RARα expression-induced NB disruption in APL development, and also of the importance of NB re-formation for an effective response to targeted therapy. Our data also underline the significant contribution of Pml NBs to the effectiveness of DNA damage repair processes, and the manner in which their disruption, mediated by the PML-RARα oncoprotein, can assist APL pathogenesis.

ACKNOWLEDGMENTS

We are indebted to all members of the Biomedical Research Centre (BRC) Flow Cytometry Core Facility, and particularly to Pj Chana and Dr Susanne Heck. We would like to thank Dr Alka Saxena of the BRC Genomics Core Facility, Dr Emanuele de Rinaldis and Dr Venu Pullabhatla of the BRC Bioinformatics Core Facility and Prof Michael Simpson (King's College London) for their support in whole-exome sequencing analysis. We are indebted to Ian Kesterton (Viapath – Cytogenetics, Guy's Hospital, London) for his help with cytogenetics analysis. We also thank staff of the Biological Services Units (FWB and NHH) at King's College London for excellent animal care.

This work was supported by a specialist program grant from Bloodwise (13043; previously called Leukaemia and Lymphoma Research) and King's College London. All BRC facilities are funded by the National Institute for Health Research (NIHR) Biomedical Research Centre based at Guy's and St Thomas' NHS Foundation Trust and King's College London. In addition, this work was supported by grant R01-CA95274 from the National Cancer Institute of the United States of America.

The authors would also like to deeply and gratefully acknowledge the central contributions, unwavering support, inspiring scientific leadership, and friendship of Prof David Grimwade without whom this work could not have been completed.

CONFLICT-OF-INTEREST DISCLOSURE

The authors declare no competing financial interests.

AUTHORSHIP CONTRIBUTIONS

E.V. designed, performed, analyzed and interpreted experiments, and supervised the study. E.M. performed experiments. E.W.S. generated the knock-in mouse model. A.J. performed whole-exome sequencing analysis. C.J.P. performed post-mortem examinations. R.K.H. performed statistical analysis on mouse cohorts. P.S. and S.C.K. provided essential reagents, and mouse models. E.S. and D.G. conceived the initial project, and supervised the study. Manuscript was prepared by E.V., E.S. and D.G. with assistance from the other authors.

REFERENCES

1. Borrow J, Goddard AD, Sheer D, Solomon E. Molecular analysis of acute promyelocytic leukemia breakpoint cluster region on chromosome 17. *Science*. 1990;249(4976):1577-1580.
2. Goddard AD, Borrow J, Freemont PS, Solomon E. Characterization of a zinc finger gene disrupted by the t(15;17) in acute promyelocytic leukemia. *Science*. 1991;254(5036):1371-1374.
3. Lallemand-Breitenbach V, de The H. PML nuclear bodies. *Cold Spring Harb Perspect Biol*. 2010;2(5):a000661.
4. Degos L, Dombret H, Chomienne C, et al. All-trans-retinoic acid as a differentiating agent in the treatment of acute promyelocytic leukemia. *Blood*. 1995;85(10):2643-2653.
5. Chen GQ, Zhu J, Shi XG, et al. In vitro studies on cellular and molecular mechanisms of arsenic trioxide (As2O3) in the treatment of acute promyelocytic leukemia: As2O3 induces NB4 cell apoptosis with downregulation of Bcl-2 expression and modulation of PML-RAR alpha/PML proteins. *Blood*. 1996;88(3):1052-1061.
6. Shao W, Fanelli M, Ferrara FF, et al. Arsenic trioxide as an inducer of apoptosis and loss of PML/RAR alpha protein in acute promyelocytic leukemia cells. *J Natl Cancer Inst*. 1998;90(2):124-133.
7. Burnett AK, Russell NH, Hills RK, et al. Arsenic trioxide and all-trans retinoic acid treatment for acute promyelocytic leukaemia in all risk groups (AML17): results of a randomised, controlled, phase 3 trial. *The Lancet Oncology*. 2015;16(13):1295-1305.
8. Kastner P, Perez A, Lutz Y, et al. Structure, localization and transcriptional properties of two classes of retinoic acid receptor alpha fusion proteins in acute promyelocytic leukemia (APL): structural similarities with a new family of oncoproteins. *EMBO J*. 1992;11(2):629-642.
9. Jensen K, Shiels C, Freemont PS. PML protein isoforms and the RBCC/TRIM motif. *Oncogene*. 2001;20(49):7223-7233.
10. Kentsis A, Gordon RE, Borden KL. Self-assembly properties of a model RING domain. *Proc Natl Acad Sci U S A*. 2002;99(2):667-672.
11. Wang ZG, Delva L, Gaboli M, et al. Role of PML in cell growth and the retinoic acid pathway. *Science*. 1998;279(5356):1547-1551.
12. Ishov AM, Sotnikov AG, Negorev D, et al. PML is critical for ND10 formation and recruits the PML-interacting protein daxx to this nuclear structure when modified by SUMO-1. *J Cell Biol*. 1999;147(2):221-234.
13. Zhong S, Hu P, Ye TZ, Stan R, Ellis NA, Pandolfi PP. A role for PML and the nuclear body in genomic stability. *Oncogene*. 1999;18(56):7941-7947.
14. Lallemand-Breitenbach V, Zhu J, Puvion F, et al. Role of promyelocytic leukemia (PML) sumolation in nuclear body formation, 11S proteasome recruitment, and As2O3-induced PML or PML/retinoic acid receptor alpha degradation. *J Exp Med*. 2001;193(12):1361-1371.
15. Shen TH, Lin HK, Scaglioni PP, Yung TM, Pandolfi PP. The mechanisms of PML-nuclear body formation. *Mol Cell*. 2006;24(3):331-339.

16. Van Damme E, Laukens K, Dang TH, Van Ostade X. A manually curated network of the PML nuclear body interactome reveals an important role for PML-NBs in SUMOylation dynamics. *Int J Biol Sci*. 2010;6(1):51-67.
17. Zhong S, Muller S, Ronchetti S, Freemont PS, Dejean A, Pandolfi PP. Role of SUMO-1-modified PML in nuclear body formation. *Blood*. 2000;95(9):2748-2752.
18. Weidtkamp-Peters S, Lenser T, Negorev D, et al. Dynamics of component exchange at PML nuclear bodies. *J Cell Sci*. 2008;121(Pt 16):2731-2743.
19. Cheng X, Kao HY. Post-translational modifications of PML: consequences and implications. *Front Oncol*. 2012;2:210.
20. Rabellino A, Scaglioni PP. PML Degradation: Multiple Ways to Eliminate PML. *Front Oncol*. 2013;3:60.
21. Thompson LH. Recognition, signaling, and repair of DNA double-strand breaks produced by ionizing radiation in mammalian cells: the molecular choreography. *Mutat Res*. 2012;751(2):158-246.
22. Jansen JH, Mahfoudi A, Rambaud S, Lavau C, Wahli W, Dejean A. Multimeric complexes of the PML-retinoic acid receptor alpha fusion protein in acute promyelocytic leukemia cells and interference with retinoid and peroxisome-proliferator signaling pathways. *Proc Natl Acad Sci U S A*. 1995;92(16):7401-7405.
23. Kogan SC, Hong SH, Shultz DB, Privalsky ML, Bishop JM. Leukemia initiated by PMLRARalpha: the PML domain plays a critical role while retinoic acid-mediated transactivation is dispensable. *Blood*. 2000;95(5):1541-1550.
24. Dyck JA, Maul GG, Miller WH, Jr., Chen JD, Kakizuka A, Evans RM. A novel macromolecular structure is a target of the promyelocyte-retinoic acid receptor oncoprotein. *Cell*. 1994;76(2):333-343.
25. de The H, Chen Z. Acute promyelocytic leukaemia: novel insights into the mechanisms of cure. *Nat Rev Cancer*. 2010;10(11):775-783.
26. Lallemand-Breitenbach V, Jeanne M, Benhenda S, et al. Arsenic degrades PML or PML-RARalpha through a SUMO-triggered RNF4/ubiquitin-mediated pathway. *Nat Cell Biol*. 2008;10(5):547-555.
27. Wojiski S, Guibal FC, Kindler T, et al. PML-RARalpha initiates leukemia by conferring properties of self-renewal to committed promyelocytic progenitors. *Leukemia*. 2009;23(8):1462-1471.
28. Nasr R, Guillemin MC, Ferhi O, et al. Eradication of acute promyelocytic leukemia-initiating cells through PML-RARA degradation. *Nat Med*. 2008;14(12):1333-1342.
29. Cappella P, Gasparri F, Pulici M, Moll J. A novel method based on click chemistry, which overcomes limitations of cell cycle analysis by classical determination of BrdU incorporation, allowing multiplex antibody staining. *Cytometry A*. 2008;73(7):626-636.
30. Seluanov A, Mittelman D, Pereira-Smith OM, Wilson JH, Gorbunova V. DNA end joining becomes less efficient and more error-prone during cellular senescence. *Proc Natl Acad Sci U S A*. 2004;101(20):7624-7629.
31. Mao Z, Jiang Y, Liu X, Seluanov A, Gorbunova V. DNA Repair by Homologous Recombination, But Not by Nonhomologous End Joining, Is Elevated in Breast Cancer Cells. *Neoplasia*. 2009;11(7):683-IN683.
32. Mohrin M, Bourke E, Alexander D, et al. Hematopoietic stem cell quiescence promotes error-prone DNA repair and mutagenesis. *Cell Stem Cell*. 2010;7(2):174-185.

33. Lin RJ, Evans RM. Acquisition of oncogenic potential by RAR chimeras in acute promyelocytic leukemia through formation of homodimers. *Mol Cell*. 2000;5(5):821-830.
34. Sternsdorf T, Phan VT, Maunakea ML, et al. Forced retinoic acid receptor alpha homodimers prime mice for APL-like leukemia. *Cancer Cell*. 2006;9(2):81-94.
35. Borden KL, Boddy MN, Lally J, et al. The solution structure of the RING finger domain from the acute promyelocytic leukaemia proto-oncoprotein PML. *EMBO J*. 1995;14(7):1532-1541.
36. Quimby BB, Yong-Gonzalez V, Anan T, Strunnikov AV, Dasso M. The promyelocytic leukemia protein stimulates SUMO conjugation in yeast. *Oncogene*. 2006;25(21):2999-3005.
37. Duprez E, Saurin AJ, Desterro JM, et al. SUMO-1 modification of the acute promyelocytic leukaemia protein PML: implications for nuclear localisation. *J Cell Sci*. 1999;112 (Pt 3):381-393.
38. Zhong S, Salomoni P, Ronchetti S, Guo A, Ruggero D, Pandolfi PP. Promyelocytic leukemia protein (PML) and Daxx participate in a novel nuclear pathway for apoptosis. *J Exp Med*. 2000;191(4):631-640.
39. Kamitani T, Kito K, Nguyen HP, Wada H, Fukuda-Kamitani T, Yeh ET. Identification of three major sentrinization sites in PML. *J Biol Chem*. 1998;273(41):26675-26682.
40. Brown D, Kogan S, Lagasse E, et al. A PMLRARalpha transgene initiates murine acute promyelocytic leukemia. *Proc Natl Acad Sci U S A*. 1997;94(6):2551-2556.
41. Grisolano JL, Wesselschmidt RL, Pelicci PG, Ley TJ. Altered myeloid development and acute leukemia in transgenic mice expressing PML-RAR alpha under control of cathepsin G regulatory sequences. *Blood*. 1997;89(2):376-387.
42. He LZ, Tribioli C, Rivi R, et al. Acute leukemia with promyelocytic features in PML/RARalpha transgenic mice. *Proc Natl Acad Sci U S A*. 1997;94(10):5302-5307.
43. Ablain J, de The H. Revisiting the differentiation paradigm in acute promyelocytic leukemia. *Blood*. 2011;117(22):5795-5802.
44. Zimonjic DB, Pollock JL, Westervelt P, Popescu NC, Ley TJ. Acquired, nonrandom chromosomal abnormalities associated with the development of acute promyelocytic leukemia in transgenic mice. *Proc Natl Acad Sci U S A*. 2000;97(24):13306-13311.
45. Le Beau MM, Bitts S, Davis EM, Kogan SC. Recurring chromosomal abnormalities in leukemia in PML-RARA transgenic mice parallel human acute promyelocytic leukemia. *Blood*. 2002;99(8):2985-2991.
46. Wartman LD, Larson DE, Xiang Z, et al. Sequencing a mouse acute promyelocytic leukemia genome reveals genetic events relevant for disease progression. *J Clin Invest*. 2011;121(4):1445-1455.
47. Riva L, Ronchini C, Bodini M, et al. Acute promyelocytic leukemias share cooperative mutations with other myeloid-leukemia subgroups. *Blood Cancer J*. 2013;3:e147.
48. Ibanez M, Carbonell-Caballero J, Garcia-Alonso L, et al. The Mutational Landscape of Acute Promyelocytic Leukemia Reveals an Interacting Network of Co-Occurrences and Recurrent Mutations. *PLoS One*. 2016;11(2):e0148346.
49. Welch JS, Ley TJ, Link DC, et al. The origin and evolution of mutations in acute myeloid leukemia. *Cell*. 2012;150(2):264-278.

50. Cancer Genome Atlas Research N. Genomic and epigenomic landscapes of adult de novo acute myeloid leukemia. *N Engl J Med*. 2013;368(22):2059-2074.
51. Ivey A, Hills RK, Simpson MA, et al. Assessment of Minimal Residual Disease in Standard-Risk AML. *N Engl J Med*. 2016;374(5):422-433.
52. Jacoby MA, Walter MJ. Detection of copy number alterations in acute myeloid leukemia and myelodysplastic syndromes. *Expert Rev Mol Diagn*. 2012;12(3):253-264.
53. Gollner S, Oellerich T, Agrawal-Singh S, et al. Loss of the histone methyltransferase EZH2 induces resistance to multiple drugs in acute myeloid leukemia. *Nat Med*. 2017;23(1):69-78.
54. Yeung PL, Denissova NG, Nasello C, Hakhverdyan Z, Chen JD, Brenneman MA. Promyelocytic leukemia nuclear bodies support a late step in DNA double-strand break repair by homologous recombination. *J Cell Biochem*. 2012;113(5):1787-1799.
55. Schwertman P, Bekker-Jensen S, Mailand N. Regulation of DNA double-strand break repair by ubiquitin and ubiquitin-like modifiers. *Nat Rev Mol Cell Biol*. 2016;17(6):379-394.
56. Bischof O, Kim SH, Irving J, Beresten S, Ellis NA, Campisi J. Regulation and localization of the Bloom syndrome protein in response to DNA damage. *J Cell Biol*. 2001;153(2):367-380.
57. Occhionorelli M, Santoro F, Pallavicini I, et al. The self-association coiled-coil domain of PML is sufficient for the oncogenic conversion of the retinoic acid receptor (RAR) alpha. *Leukemia*. 2011;25(5):814-820.
58. Korf K, Wodrich H, Haschke A, et al. The PML domain of PML-RARalpha blocks senescence to promote leukemia. *Proc Natl Acad Sci U S A*. 2014;111(33):12133-12138.
59. Doucas V, Tini M, Egan DA, Evans RM. Modulation of CREB binding protein function by the promyelocytic (PML) oncoprotein suggests a role for nuclear bodies in hormone signaling. *Proc Natl Acad Sci U S A*. 1999;96(6):2627-2632.
60. Zhong S, Delva L, Rachez C, et al. A RA-dependent, tumour-growth suppressive transcription complex is the target of the PML-RARalpha and T18 oncoproteins. *Nat Genet*. 1999;23(3):287-295.
61. Ablain J, Leiva M, Peres L, Fonsart J, Anthony E, de The H. Uncoupling RARA transcriptional activation and degradation clarifies the bases for APL response to therapies. *J Exp Med*. 2013;210(4):647-653.
62. El Hajj H, Dassouki Z, Berthier C, et al. Retinoic acid and arsenic trioxide trigger degradation of mutated NPM1, resulting in apoptosis of AML cells. *Blood*. 2015;125(22):3447-3454.
63. Martelli MP, Gionfriddo I, Mezzasoma F, et al. Arsenic trioxide and all-trans retinoic acid target NPM1 mutant oncoprotein levels and induce apoptosis in NPM1-mutated AML cells. *Blood*. 2015;125(22):3455-3465.
64. Matthay KK, Reynolds CP, Seeger RC, et al. Long-term results for children with high-risk neuroblastoma treated on a randomized trial of myeloablative therapy followed by 13-cis-retinoic acid: a children's oncology group study. *J Clin Oncol*. 2009;27(7):1007-1013.
65. Liu Z, Ren G, Shangguan C, et al. ATRA inhibits the proliferation of DU145 prostate cancer cells through reducing the methylation level of HOXB13 gene. *PLoS One*. 2012;7(7):e40943.
66. Chen MC, Hsu SL, Lin H, Yang TY. Retinoic acid and cancer treatment. *Biomedicine (Taipei)*. 2014;4:22.

67. Centritto F, Paroni G, Bolis M, et al. Cellular and molecular determinants of all-trans retinoic acid sensitivity in breast cancer: Luminal phenotype and RARalpha expression. *EMBO Mol Med*. 2015;7(7):950-972.
68. Yan Y, Li Z, Xu X, et al. All-trans retinoic acids induce differentiation and sensitize a radioresistant breast cancer cells to chemotherapy. *BMC Complement Altern Med*. 2016;16:113.
69. di Masi A, Cilli D, Berardinelli F, et al. PML nuclear body disruption impairs DNA double-strand break sensing and repair in APL. *Cell Death Dis*. 2016;7:e2308.
70. Munch S, Weidtkamp-Peters S, Klement K, et al. The tumor suppressor PML specifically accumulates at RPA/Rad51-containing DNA damage repair foci but is nonessential for DNA damage-induced fibroblast senescence. *Mol Cell Biol*. 2014;34(10):1733-1746.
71. Viale A, De Franco F, Orleth A, et al. Cell-cycle restriction limits DNA damage and maintains self-renewal of leukaemia stem cells. *Nature*. 2009;457(7225):51-56.
72. Le Beau MM, Davis EM, Patel B, Phan VT, Sohal J, Kogan SC. Recurring chromosomal abnormalities in leukemia in PML-RARA transgenic mice identify cooperating events and genetic pathways to acute promyelocytic leukemia. *Blood*. 2003;102(3):1072-1074.
73. Jackson SP, Durocher D. Regulation of DNA damage responses by ubiquitin and SUMO. *Mol Cell*. 2013;49(5):795-807.
74. Ouyang KJ, Woo LL, Zhu J, Huo D, Matunis MJ, Ellis NA. SUMO modification regulates BLM and RAD51 interaction at damaged replication forks. *PLoS Biol*. 2009;7(12):e1000252.
75. Dou H, Huang C, Singh M, Carpenter PB, Yeh ET. Regulation of DNA repair through deSUMOylation and SUMOylation of replication protein A complex. *Mol Cell*. 2010;39(3):333-345.
76. Galanty Y, Belotserkovskaya R, Coates J, Jackson SP. RNF4, a SUMO-targeted ubiquitin E3 ligase, promotes DNA double-strand break repair. *Genes Dev*. 2012;26(11):1179-1195.
77. Panier S, Boulton SJ. Double-strand break repair: 53BP1 comes into focus. *Nat Rev Mol Cell Biol*. 2014;15(1):7-18.
78. Galanty Y, Belotserkovskaya R, Coates J, Polo S, Miller KM, Jackson SP. Mammalian SUMO E3-ligases PIAS1 and PIAS4 promote responses to DNA double-strand breaks. *Nature*. 2009;462(7275):935-939.
79. Chapman JR, Barral P, Vannier JB, et al. RIF1 is essential for 53BP1-dependent nonhomologous end joining and suppression of DNA double-strand break resection. *Mol Cell*. 2013;49(5):858-871.
80. Bouwman P, Aly A, Escandell JM, et al. 53BP1 loss rescues BRCA1 deficiency and is associated with triple-negative and BRCA-mutated breast cancers. *Nat Struct Mol Biol*. 2010;17(6):688-695.
81. Bunting SF, Callen E, Wong N, et al. 53BP1 inhibits homologous recombination in Brca1-deficient cells by blocking resection of DNA breaks. *Cell*. 2010;141(2):243-254.
82. Zimmermann M, de Lange T. 53BP1: pro choice in DNA repair. *Trends Cell Biol*. 2014;24(2):108-117.
83. Feng L, Li N, Li Y, et al. Cell cycle-dependent inhibition of 53BP1 signaling by BRCA1. *Cell Discov*. 2015;1:15019.
84. Ochs F, Somyajit K, Altmeyer M, Rask MB, Lukas J, Lukas C. 53BP1 fosters fidelity of homology-directed DNA repair. *Nat Struct Mol Biol*. 2016;23(8):714-721.

85. Park MA, Seok YJ, Jeong G, Lee JS. SUMO1 negatively regulates BRCA1-mediated transcription, via modulation of promoter occupancy. *Nucleic Acids Res*. 2008;36(1):263-283.
86. Morris JR, Boutell C, Keppler M, et al. The SUMO modification pathway is involved in the BRCA1 response to genotoxic stress. *Nature*. 2009;462(7275):886-890.
87. Vialter A, Vincent A, Demidem A, et al. Cell cycle-dependent conjugation of endogenous BRCA1 protein with SUMO-2/3. *Biochim Biophys Acta*. 2011;1810(4):432-438.

LEGENDS

Figure 1. Pml$^{C62A/C65A}$ expression induces mislocalization of NB constituents, Pml SUMOylation deficiency, and expansion of the LSK compartment. (A) Representative confocal microscopy images are presented for Pml (green), Daxx, Cbp and Sumo-1 (red) staining in Pml^{WT}, Pml$^{C62A/C65A}$, and Pml$^{-/-}$ MEFs. Nuclei were counterstained with DAPI (blue). Scale bar, 10 μm. (B) Expression levels demonstrated by Western blot analysis of whole cell lysates extracted from Pml^{WT}, Pml$^{C62A/C65A}$, and Pml$^{-/-}$ MEFs. The asterisk indicates a non-specific band. Tubulin was used as loading control. (C) Representative images of DAXX (red) and PML (green) staining in NB4 cells treated with DMSO (vehicle control) or ATRA (1μM). Nuclei were counterstained with DAPI (blue). Scale bar, 10 μm. (D) MEFs were treated with or without ATO (1μM) for 1 h, as indicated, followed by immunoprecipitation (IP) by control IgG (CTRL) or with antibodies against the indicated protein. The immunoprecipitates were analyzed by immunoblot (IB) with an anti-Pml antibody in order to reveal the SUMOylated or ubiquitinated forms of Pml. Data shown are representative of three independent experiments. (E) Relative number of Lin$^-$Sca-1$^+$c-Kit$^+$ (LSK) cells in BM at 8 weeks (n≥3). (F) Cell cycle phase distribution of LSK cells labeled with Click-iT EdU in vivo (n≥3). (G) Representative dot plots of cell cycle status of LSK population. (E and F) Two-tailed unpaired Student's *t* test analyses were performed.

Figure 2. Pml NB disruption improves induction of APL. (A) Kaplan-Meier curve showing cumulative incidence of APL in Pml^{WT} (n=249), Pml$^{C62A/C65A}$ (n=251), Pml^{WT}+p50-RARα (n=252), and Pml$^{C62A/C65A}$+p50-RARα (n=251). (B) Top panels:

Representative pictures of blood smear of moribund $Pml^{C62A/C65A}$+p50-RARα mice showing hyperleukocytosis (May-Grünwald Giemsa staining). Bottom panel: Representative spleens of Pml^{WT} healthy control and $Pml^{C62A/C65A}$+p50-RARα leukemic mice. (C) Kaplan-Meier survival curve of mouse primary recipients transplanted with Pml^{WT}+p50-RARα (n=14) and $Pml^{C62A/C65A}$+p50-RARα (n=8) leukemic BM cells, from three independent leukemias each. Mouse recipients transplanted with PML-RARα leukemic BM cells (n=13) from three independent leukemic samples. This graph represents pooled data from two independent experiments. (A and C) Log-rank tests were used to compare survival curves.

Figure 3. Response to ATRA treatment is compromised when Pml NBs are disrupted. (A) Differentiation of BM cells from secondary recipients determined by in vitro NBT assay following treatment with DMSO (vehicle control) or ATRA (1μM) (n≥4). A minimum of 1100 cells were counted per sample using the Nikon NIS Elements C software. Two-tailed unpaired Student's *t* test analysis was performed. (B) Representative contour plots of leukemic blasts treated with DMSO (vehicle control) or ATRA (1μM) for the myeloid differentiation markers CD11b and Gr1. (C) Survival of secondary recipients treated with ATRA (5mg) or placebo pellets from day 7 post-transplantation (n≥5). This graph represents pooled data from three independent experiments. Log-rank test was used. T= Transplantation; I= Implantation.

Figure 4. Efficiency of NHEJ and HR altered by Pml NB disruption. (A) Efficiency of NHEJ-C (Compatible DNA ends), NHEJ-I (Incompatible DNA ends), and HR pathways in primary MEFs (n=3). The efficiency of repair was measured by

quantification of GFP fluorescence expression, which can only occur when linearized plasmids are accurately ligated (NHEJ-C) or repaired (NHEJ-I and HR). (B) Efficiency of NHEJ-C in lineage-depleted BM cells (n≥5). (C) Efficiency of NHEJ-C, NHEJ-I and HR in U937-Empty vector and U937-PR9 cell lines, 48 h after $ZnSO_4$ treatment for induction of PML-RARα expression (n=4). Western blot analysis of whole cell lysates from U937-Empty vector and U937-PR9 cell lines treated with (+) or without (-) $ZnSO_4$ confirming PML-RARα expression. Tubulin was used as loading control. (A to C) Two-tailed unpaired Student's *t* test analyses were performed. (D) Percentage of chromosomal aberrations (breaks, gaps and rearrangements) in MEFs at the indicated time post-IR (n>40 metaphase spreads from three independent experiments). Representative images inset of a chromatid rearrangement and a chromatid gap. (E) Sister chromatid exchanges (SCEs) rate per chromosome in MEFs, non-treated or treated with IR (n>30 metaphase spreads from three independent experiments). Representative image inset of SCEs. (D and E) Two-tailed Mann-Whitney U-test was used.

Figure 5. Elevated co-localization between 53BP1 and Brca1 foci in $Pml^{C62A/C65A}$ cells. (A) Ratio of 53BP1 foci in MEFs over a 24 h time course following IR exposure (n=3 per time point). Two-tailed unpaired Student's *t* test analysis was performed. *, $P < 0.05$. (B) Representative images of irradiated MEFs immunostained for 53BP1 (red), γH2AX (green) and DAPI (blue). Scale bar, 10 μm. (C) Quantification of 53BP1 and Brca1 foci co-localization 1 h post-IR in MEFs from three independent experiments. Only cells co-expressing 53BP1 and Brca1 foci were counted. Significance was assessed by two-tailed Mann-Whitney U-test. (D) Representative

images of irradiated MEFs immunostained for 53BP1 (green), Brca1 (red) and DAPI (blue). Scale bar, 10 μm.

Figure 6. Reduced co-localization between Rad51 and γH2AX foci in Pml$^{C62A/C65A}$ and Pml$^{-/-}$ cells. (A) Representative images of Pml^{WT}, Pml$^{-/-}$ and Pml$^{C62A/C65A}$ MEFs overexpressing GFP-Blm (GFP-Blm, green; DAPI, blue). Scale bar, 10 μm. (B) Representative co-staining images of Blm/Pml in Pml^{WT} MEF overexpressing GFP-Blm (GFP-Blm, green; Pml, red; DAPI, blue). Scale bar, 10 μm. (C) Ratio of GFP-Blm foci in MEFs (n=3). (D) Ratio of Rad51 foci in MEFs over a 24 h time course following IR exposure (n=3 per time point). (C and D) Two-tailed unpaired Student's *t* test analyses were performed. *, $P < 0.05$; **, $P < 0.01$. (E) Representative images of irradiated MEFs immunostained for Rad51 (red), γH2AX (green) and DAPI (blue). Scale bar, 10 μm. (F) Co-immunoprecipitation experiments. Cells treated without (-) or 1 h post-IR (+) exposure were lysed and immunoprecipitated (IP) with anti-Rad51 antibody and immunoblotted with anti-γH2AX antibody. Input is shown in the lower panels. The blots shown are representative of three independent experiments.

Figure 1.

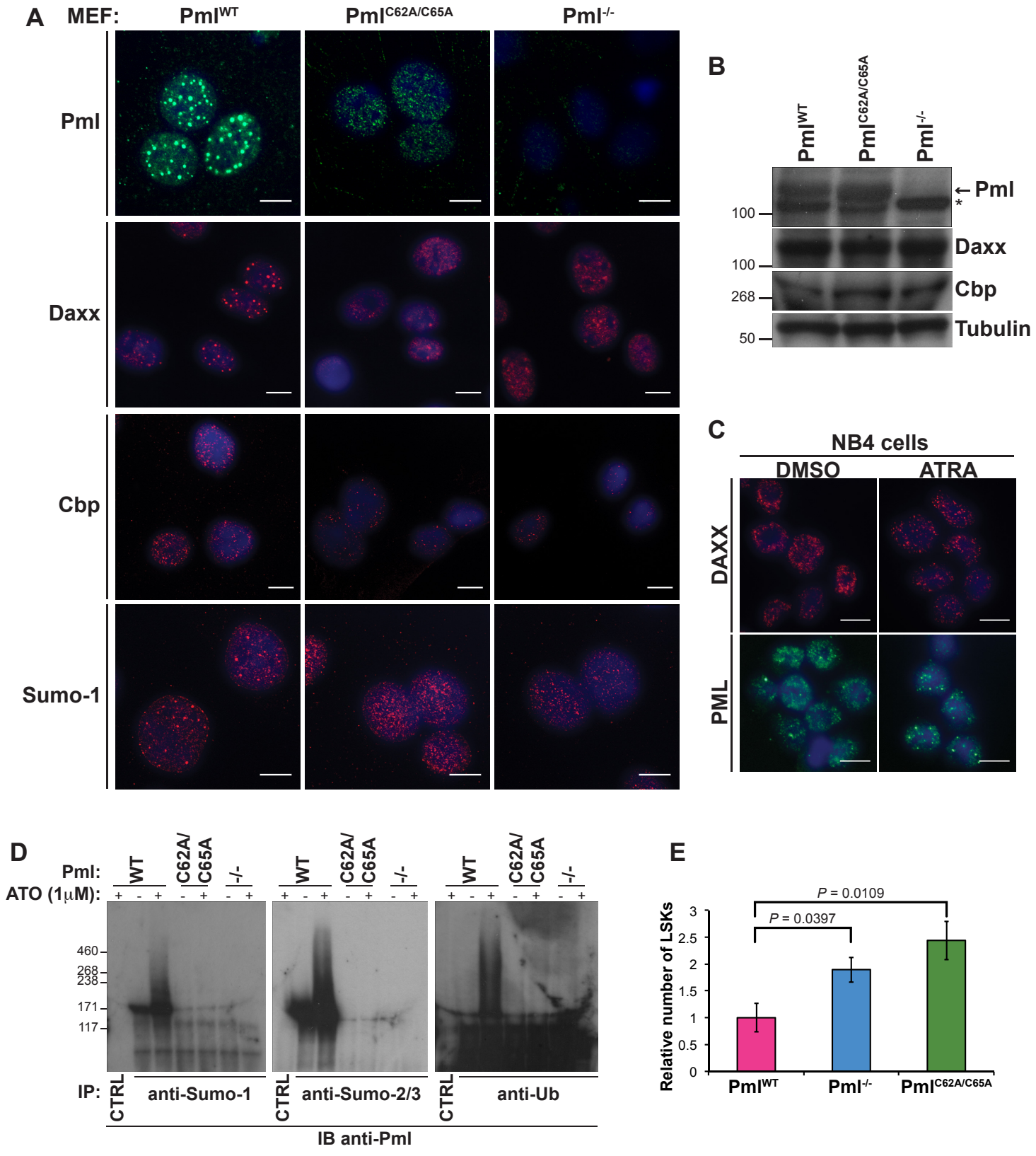

Voisset et al., 2017

Figure 2.

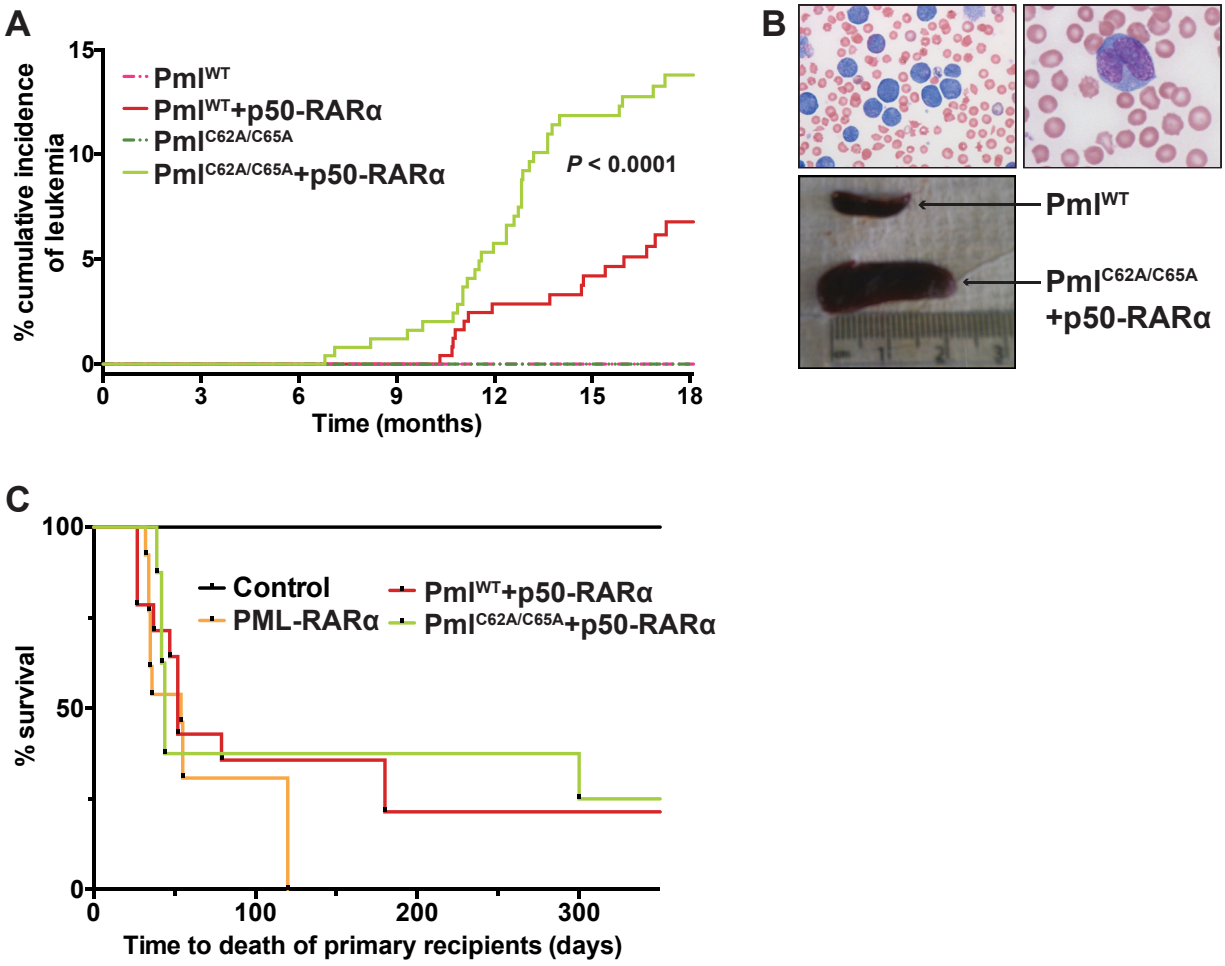

Voisset et al., 2017

Figure 3.

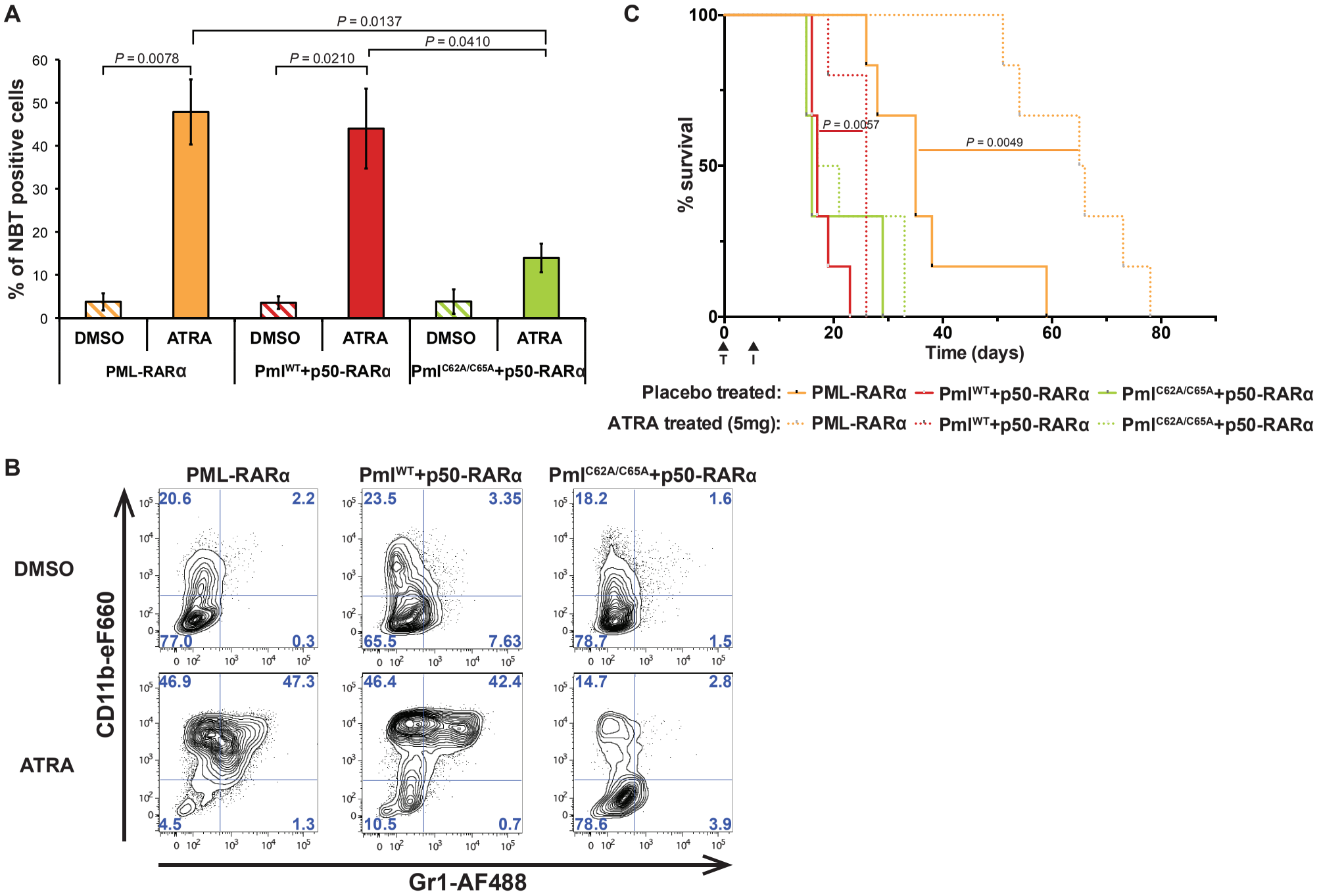

Voisset et al., 2017

Figure 4.

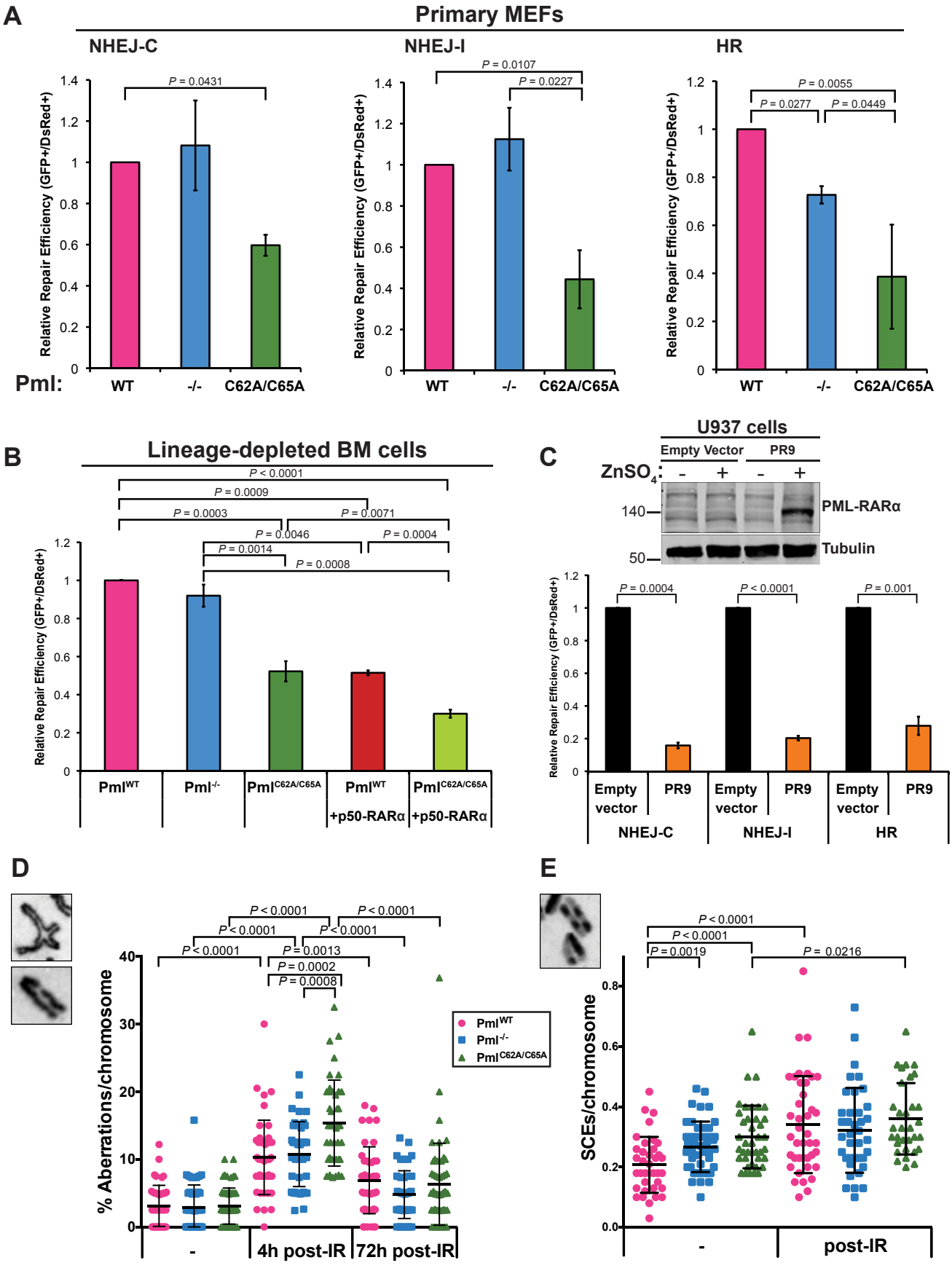

Voisset et al., 2017

Figure 5.

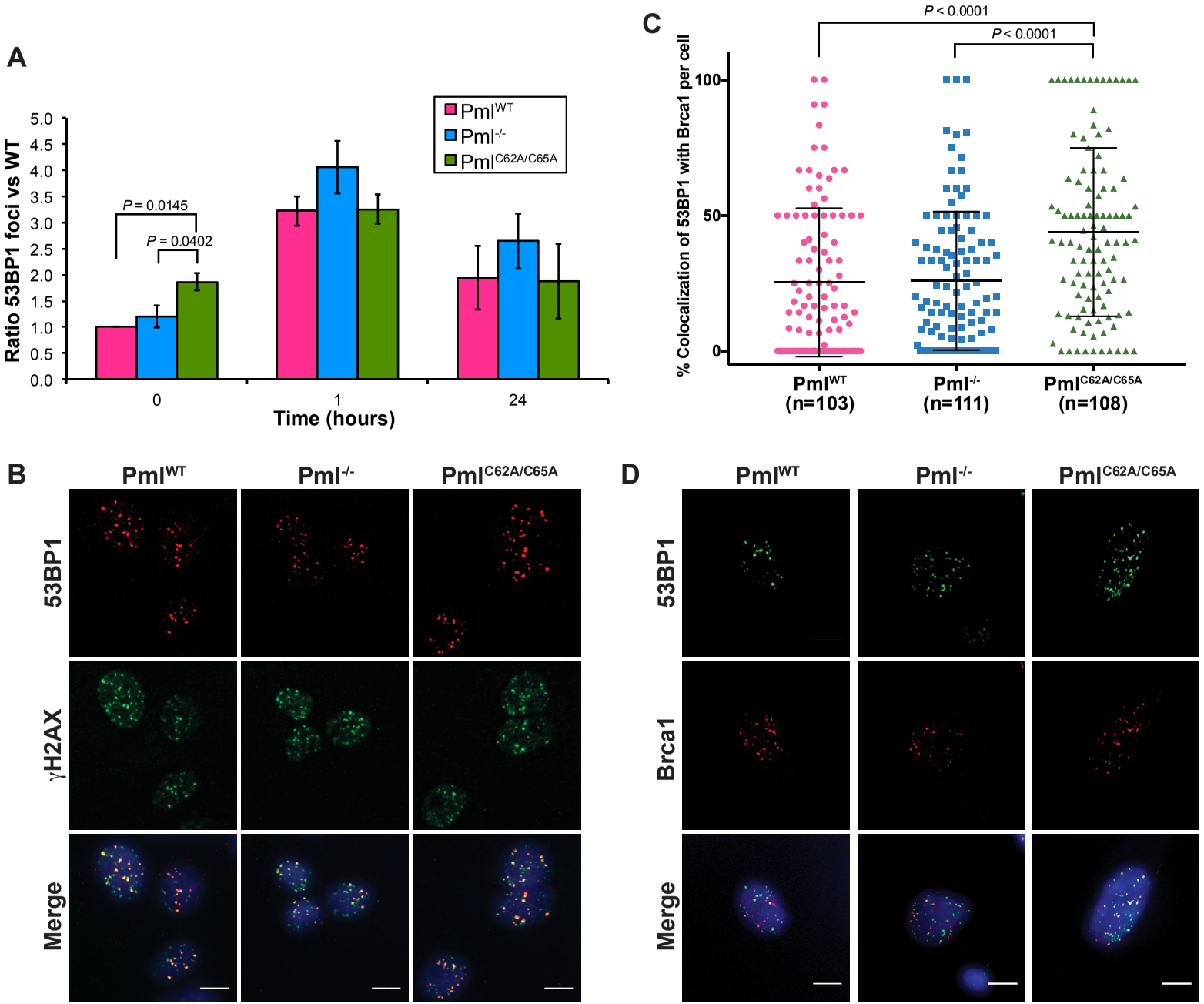

Voisset et al., 2017

Figure 6.

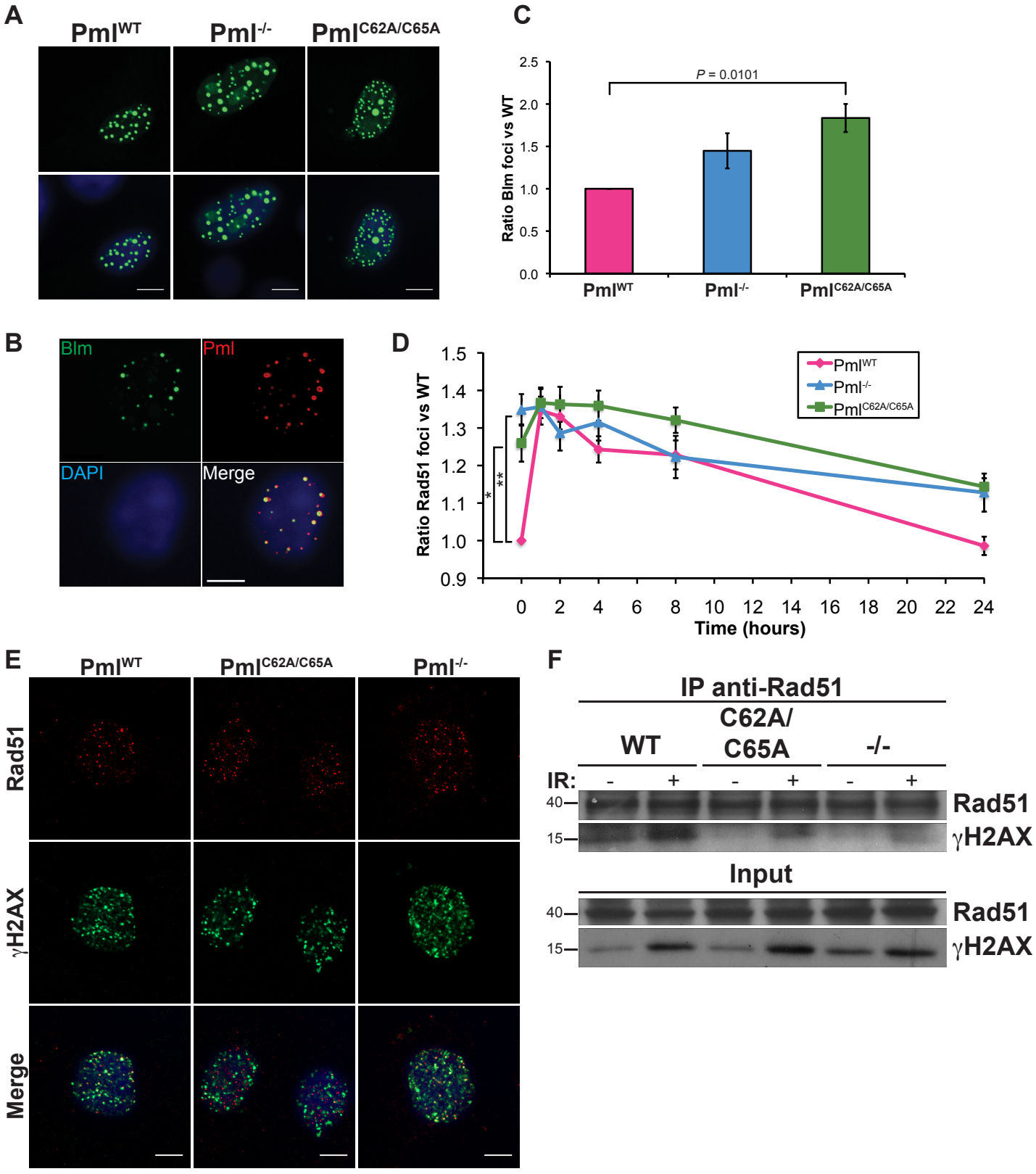

Voisset et al., 2017